



**HAL**  
open science

## Molecularly imprinted polypyrrole based sensor for the detection of SARS-CoV-2 spike glycoprotein

Vilma Ratautaite, Raimonda Boguzaitė, Ernestas Brazys, Almira Ramanaviciene, Evaldas Ciplys, Mindaugas Juozapaitis, Rimantas Slibinskas, Mikhael Bechelany, Arunas Ramanavicius

### ► To cite this version:

Vilma Ratautaite, Raimonda Boguzaitė, Ernestas Brazys, Almira Ramanaviciene, Evaldas Ciplys, et al.. Molecularly imprinted polypyrrole based sensor for the detection of SARS-CoV-2 spike glycoprotein. *Electrochimica Acta*, 2022, 403, pp.139581. 10.1016/j.electacta.2021.139581 . hal-03851962

**HAL Id: hal-03851962**

**<https://hal.umontpellier.fr/hal-03851962v1>**

Submitted on 14 Nov 2022

**HAL** is a multi-disciplinary open access archive for the deposit and dissemination of scientific research documents, whether they are published or not. The documents may come from teaching and research institutions in France or abroad, or from public or private research centers.

L'archive ouverte pluridisciplinaire **HAL**, est destinée au dépôt et à la diffusion de documents scientifiques de niveau recherche, publiés ou non, émanant des établissements d'enseignement et de recherche français ou étrangers, des laboratoires publics ou privés.

# Molecularly Imprinted Polypyrrole based Sensor for the Detection of SARS-CoV-2 Spike Glycoprotein

Vilma Ratautaite<sup>1,3</sup>, Raimonda Boguzaitė<sup>1,3</sup>, Ernestas Brazys<sup>3</sup>, Almira Ramanaviciene<sup>3</sup>, Evaldas Ciplys<sup>3,4</sup>, Mindaugas Juozapaitis<sup>3,4</sup>, Rimantas Slibinskas<sup>3,4</sup>, Mikhael Bechelany<sup>5</sup>, Arunas Ramanavicius<sup>2,3\*</sup>

<sup>1</sup> Laboratory of Nanotechnology, Department of Functional Materials and Electronics, Center for Physical Sciences and Technology, Sauletekio av. 3, Vilnius LT-10257, Lithuania;

<sup>2</sup> Department of Physical Chemistry, Institute of Chemistry, Faculty of Chemistry and Geosciences, Vilnius University, Naugarduko str. 24, Vilnius LT-03225 Lithuania;

<sup>3</sup> NanoTechnas – Center of Nanotechnology and Materials Science at Faculty of Chemistry and Geosciences, Vilnius University, Naugarduko str. 24, LT-03225, Vilnius, Lithuania;

<sup>4</sup> Institute of Biotechnology, Life Sciences Center, Vilnius University, Sauletekio av. 7, LT-10257 Vilnius, Lithuania;

<sup>5</sup> Institut Européen des Membranes, Montpellier University 2, Place Eugène Bataillon, 34095 Montpellier Cedex 5, France.

\* Corresponding author: Prof. habil. dr. Arūnas Ramanavičius (Vilnius University) [arunas.ramanavicius@chf.vu.lt](mailto:arunas.ramanavicius@chf.vu.lt)

## Abstract

This study describes the application of a polypyrrole-based sensor for the determination of SARS-CoV-2-S spike glycoprotein. The SARS-CoV-2-S spike glycoprotein is a spike protein of the coronavirus SARS-CoV-2 that recently caused the worldwide spread of COVID-19 disease. This study is dedicated to the development of an electrochemical determination method based on the application of molecularly imprinted polymer technology. The electrochemical sensor was designed by molecular imprinting of polypyrrole (Ppy) with SARS-CoV-2-S spike glycoprotein (MIP-Ppy). The electrochemical sensors with MIP-Ppy and with polypyrrole without imprints (NIP-Ppy) layers were electrochemically deposited on a platinum electrode surface by a sequence of potential pulses. The performance of polymer layers was evaluated by pulsed amperometric detection (CA). According to the obtained results, a sensor based on MIP-Ppy is more sensitive to the SARS-CoV-2-S spike glycoprotein than a sensor based on NIP-Ppy. Also, the results demonstrate that the MIP-Ppy layer is more selectively interacting with SARS-CoV-2-S glycoprotein than with bovine serum

1 albumin. This proves that molecularly imprinted MIP-Ppy-based sensors might be applied for the  
2 detection of SARS-CoV-2 virus proteins.

3

4

5 **Keywords:** COVID-19; SARS-CoV-2 Spike glycoprotein; Polypyrrole (Ppy); conducting  
6 polymers; molecularly imprinted polymers (MIPs); electrochemical determination of virus  
7 proteins; thin layers.

8

## 9 **1. Introduction**

10 The severe acute respiratory syndrome coronavirus-2 (SARS-CoV-2) induced COVID-19  
11 pandemic that began in 2019 has caused drastic changes in the world. 197 countries were  
12 affected [1]: lockdowns [2], quarantine, economic problems hit the most significant part of the  
13 world, people's emotional health has deteriorated. Even at the beginning of the 2021, this  
14 pandemic is still not adequately controlled. Although the vaccines became available to society,  
15 this viral infection is still very active and the virus is rather rapidly mutating and appears in  
16 new even more infectious forms. Therefore, a much deeper understanding of the virus SARS-  
17 CoV-2 is required and rapid analytical methods that are suitable for the diagnosis of COVID-19  
18 and/or detection of virus or their parts are demanded to overcome and defeat this infection.  
19 Thus, various aspects of the virus itself [3], genome [4-7], research of the structure, function of  
20 proteins, and nucleocapsid, envelope, spike, and membrane protein interactions with drugs [8-  
21 11], and some other aspects [12, 13] were investigated. Better and easier detection methods  
22 could improve the diagnosis of viral infection and enable more efficient ways of defeating the  
23 COVID-19 pandemic. Recently, label-free protein detection has become relevant in research  
24 and clinical practice [14, 15]. The discovery and detection of biomarkers during the diagnosis  
25 of human diseases is required for biomedical purposes [15, 16].

26 In biosensors the analyte recognition elements are typically based on bio-  
27 macromolecules such as enzymes, antibodies, DNA, aptamers, etc. However, such bioanalytical  
28 systems have some limitations due to operating conditions and expensive production.  
29 Therefore, the development of artificial biorecognition-systems based on synthetic receptors  
30 and molecularly imprinted polymers (MIPs) has attracted a great interest as a potential  
31 alternative [14, 17]. Researchers have been focused on the development of a system that  
32 replicates the natural recognition process. Therefore, the interest in the development of MIPs  
33 has grown during recent years [15, 16, 18-25]. The technique of molecular imprinting allows  
34 the formation of specific molecular recognition sites that operate on the principle of

1 complementarity between the imprinted sites and the analyte. Therefore, MIPs can selectively  
2 bind the analytes of interest, which were used as templates during formation of these MIPs [14,  
3 16, 26-28]. MIPs also have some other benefits including low-cost, easy way of preparation,  
4 advanced storage stability, and rather good specificity [14, 29]. In previous studies, it was  
5 reported that various types of small molecules can be imprinted within polymers [22, 27, 30,  
6 31]. In some researches, it was demonstrated that high molecular mass biomolecules including  
7 proteins [15, 20, 21, 32-41] can be also molecularly imprinted within polymers. Polypyrrole  
8 (Ppy) is among several other polymers that can be very efficiently applied for the design of  
9 MIP-based sensors [22, 27, 30, 31, 42-45]. This is a conducting polymer, which can be easily  
10 electropolymerized and used as a polymeric matrix of MIPs for the detection of low and high  
11 molecular weight analytes [15, 42]. Electrochemical methods like cyclic voltammetry,  
12 differential pulse voltammetry, and electrochemical impedance spectroscopy were used for  
13 the detection of the proteins both on the polypyrrole modified with molecular imprints and on  
14 the unmodified in previous studies [15, 46-52]. Meanwhile, there is only few reports on the  
15 application of chronoamperometry for determination of virus-proteins [42]. In  
16 chronoamperometry the changes in the current appear in response to increase or decrease of  
17 the diffuse layer thickness at the surface of the working electrode. Therefore, the application  
18 of chronoamperometry (in pulsed amperometric mode) and the analysis of data gathered by  
19 this method using Cottrell or Anson plots are providing interesting and useful insights into the  
20 evaluation of interaction between analytes and the electrode.

21 At the moment, there are some explorations reported that are already applying MIP  
22 technology for SARS-CoV-2 [53, 54]. The development of so called 'monoclonal-type plastic  
23 antibodies' based on MIPs was described [53]. Such 'antibodies' were able to selectively bind  
24 a spike protein of the novel coronavirus SARS-CoV-2 to block its function. The obtained  
25 nanoparticles were analyzed by SDS-PAGE electrophoresis. The results of the electrophoretic  
26 analysis demonstrated promising results in the formulation of 'free-drug therapeutics' due to  
27 their ability to bind the virus spike glycoprotein and, thus, to block the infection process.  
28 According to reported results it was concluded that the 'monoclonal-type plastic antibodies'  
29 could be potentially used as free-drug therapeutics in the treatment of infection 2019-nCoV. In  
30 another research, SARS-CoV-2 nucleoprotein (ncovNP) was qualitatively and quantitatively  
31 determined by MIP-based layer on poly-m-phenylenediamine (PmPD), which was deposited  
32 on the Au-TFE electrode [54]. Cyclic voltammetry (CV) was applied for the characterization of  
33 the preparation steps of the sensor. Meanwhile, the rebinding of SARS-CoV-2 nucleoprotein on  
34 the sensors was studied by differential pulse voltammetry (DPV) in the solution of 1 M KCl

1 containing a redox probe  $K_3[Fe(CN)_6]/K_4[Fe(CN)_6]$ . The obtained results demonstrated the  
2 linear increase of the sensor response with increasing ncovNP concentration. The feasibility of  
3 sensor performance in clinical samples was tested. For this purpose they analyzed the samples  
4 prepared from nasopharyngeal swab specimens. Genetically engineered receptor-binding  
5 domain of SARS-CoV-2-RBD protein was imprinted in ortho-phenylenediamine and deposited  
6 on a macroporous gold screen-printed electrode [55].

7 The aim of recent research was to design the MIP-based sensor for the determination  
8 of SARS-CoV-2-S glycoprotein. For this purpose, Ppy layers were deposited on the working  
9 platinum electrode from the polymerization mixture containing SARS-CoV-2-S glycoprotein  
10 and pyrrole dissolved in phosphate buffered saline (PBS) solution, pH 7.4. The performance of  
11 the electrode modified by the deposited MIP-Ppy layer imprinted with SARS-CoV-2-S  
12 glycoprotein was investigated and compared with that of non-imprinted (NIP-Ppy) layer.

## 13 14 **2. Materials and methods**

### 15 **2.1. Chemicals and instrumentation**

16 Pyrrole 98% (*Alfa Aeser*, Germany),  $H_2SO_4$  (96 %) (*Lachner*, Czech Republic),  $HNO_3$ , NaOH  
17 (*Merck*, Germany),  $H_2PtCl_6$  (*Merck*, Germany), and bovine serum albumin (BSA) (*Carl Roth*,  
18 Germany) were used as received.  $KH_2PO_4$  (*Honeywell Riedel-de Haen*, Germany), NaCl, KCl, and  
19  $Na_2HPO_4$  (*Roth*, Germany) salts were used for the preparation of buffer. The detailed  
20 description of expression and purification of SARS-CoV-2-S spike glycoprotein is presented in  
21 supporting material.

22 Experiment was performed using potentiostat/galvanostat Metrohm AutoLAB model  
23  $\mu$ AutolabIII/FRA2  $\mu$ 3AUT71079 controlled by NOVA 2.1.3 software (*EcoChemie*, The  
24 Netherlands). All measurements were done in a home-made cell. The total volume of the cell  
25 was 250  $\mu$ L. Three-electrode system consisted of Pt disk with 1 mm diameter sealed in glass as  
26 the working electrode, Ag/AgCl in 3M KCl solution electrode as a reference electrode  
27 (Ag/AgCl), and Pt disk of 2 mm diameter as a counter electrode.

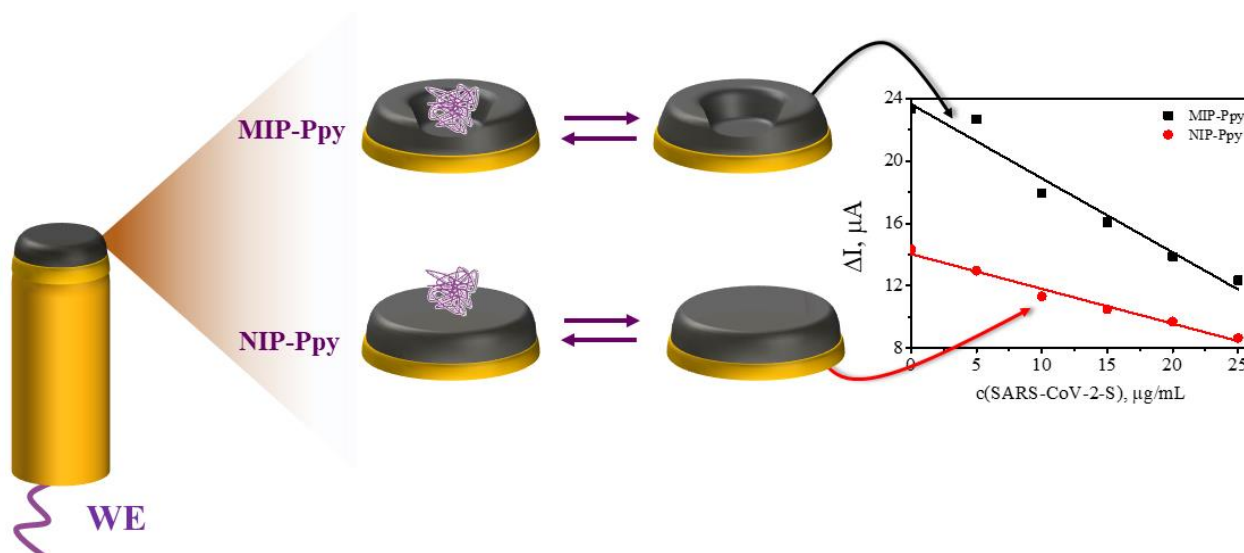
### 28 29 **2.2. Pretreatment of working electrode**

30 The working electrode was pretreated before electrochemical deposition of Ppy following the  
31 procedure described in previous studies [42, 56]. All solutions were thoroughly degassed just  
32 before use with a stream of  $N_2$ . According to this procedure, the Pt electrode was rinsed with  
33 concentrated  $HNO_3$  solution in an ultrasonic bath for 10 min, then rinsed with water and  
34 polished with alumina paste. Later, it was rinsed with water again and then with 10 M solution

1 of NaOH, thereafter – with 5 M solution of H<sub>2</sub>SO<sub>4</sub> in an ultrasonic bath for 5 min.  
2 Electrochemical cleaning of the electrode was carried out in 0.5 M H<sub>2</sub>SO<sub>4</sub> by cycling the  
3 potential for 20 times in the range between –100 mV and +1200 mV vs Ag/AgCl at a sweep rate  
4 of 100 mV s<sup>-1</sup>. The identification of the bare electrode surface was made possible by a stable  
5 indication of the cyclic voltammogram. To improve the adhesion of the Ppy layer to the  
6 electrode surface, a layer of ‘platinum black’ was deposited over the working electrode [56].  
7 Deposition of Pt clusters was performed in 5 mM solution of H<sub>2</sub>PtCl<sub>6</sub> containing 0.1 M of KCl by  
8 10 potential cycles in the range between +500 mV and –400 mV vs Ag/AgCl at a sweep rate of  
9 10 mV s<sup>-1</sup>.

### 10 2.3. The electrochemical deposition of MIP and NIP and evaluation of sensor signal

11  
12  
13



14  
15 **Fig. 1.** Schematic representation of evaluation by chronoamperometry of Pt electrode modified  
16 with non-imprinted polypyrrole (NIP-Ppy) and with molecularly imprinted polypyrrole (MIP-  
17 Ppy) with SARS-CoV-2-S glycoprotein imprints. Electrochemical measurements were  
18 performed in phosphate-buffered saline (PBS) solution, pH 7.4.

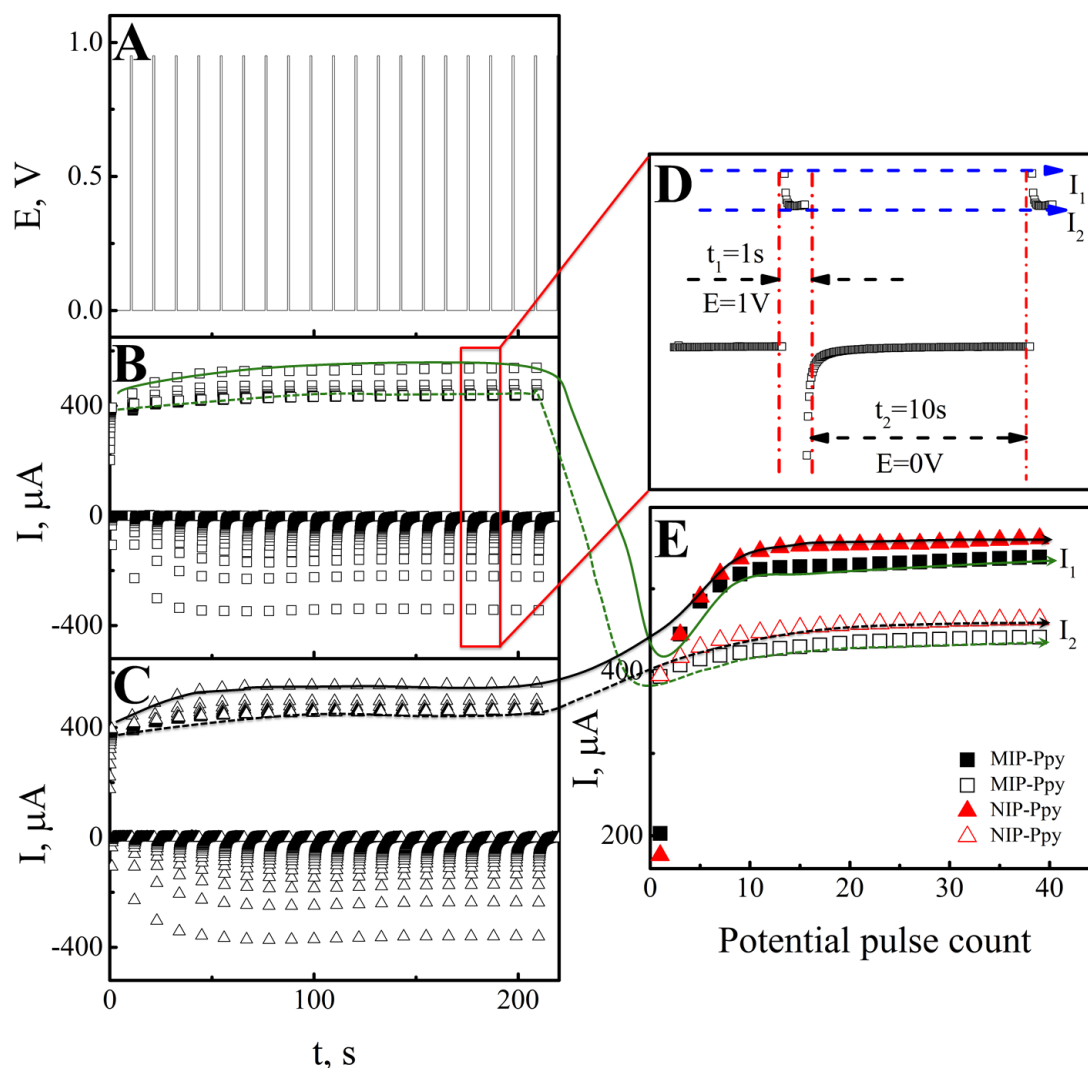
19  
20 The electrochemical deposition of the polypyrrole layer was performed in the same  
21 electrochemical cell. NIP-Ppy was electrochemically deposited from the polymerization  
22 solution containing 0.5 M solution of pyrrole in PBS. The preparation of MIP-Ppy was carried  
23 out in two steps. Step I: deposition of polymeric layer was carried out from the polymerization  
24 solution containing 0.5 M solution of pyrrole and 50 μg/mL of SARS-CoV-2-S glycoprotein all

1 dissolved in PBS solution. The polymeric layers were formed by a sequence of 20 potential  
2 pulses of +950 mV for 1 s, between these pulses 0 V potential for 10 s was applied [42, 56].  
3 Step II: the MIP-Ppy was formed when the imprinted protein molecules were extracted by  
4 incubation in 0.05 M H<sub>2</sub>SO<sub>4</sub> for 10 min. In the same way as MIP-Ppy, NIP-Ppy was also exposed  
5 to 0.05 M solution of H<sub>2</sub>SO<sub>4</sub>. MIP-Ppy and NIP-Ppy were analyzed using pulsed amperometric  
6 detection by the sequence of 10 potential pulses of +600 mV vs Ag/AgCl lasting for 2 s, between  
7 these pulses 0 V vs Ag/AgCl was applied for 2 s (Fig. 1).

8

### 9 **3. Results and discussions**

10 Electrochemical polymerization of the two types of Ppy layers was performed by a sequence  
11 of potential pulses (Fig. 2). The profile of potential pulses sequence is represented in figure 2A.  
12 Figures 2B and 2C demonstrate the currents registered during the electrochemical deposition  
13 of Ppy layer from polymerization solution containing SARS-CoV-2-S glycoprotein and Ppy layer  
14 from polymerization solution non-containing SARS-CoV-2-S glycoprotein on Pt-electrode  
15 surface.



1  
 2 **Fig. 2.** Electrochemical deposition of the polypyrrole layers on the Pt electrode: **A** – The profile  
 3 of potential applied during the sequence of potential pulses; **B** – The profile of current  
 4 registered during the deposition of Ppy layer from polymerization solution containing SARS-  
 5 CoV-2-S glycoprotein; **C** – The profile of current registered during the formation of Ppy layer  
 6 from polymerization solution non-containing SARS-CoV-2-S glycoprotein. **D** – The profile of  
 7 current registered during one potential pulse. **E** – Changes of current measured instantly after  
 8 a potential step of +950 mV.

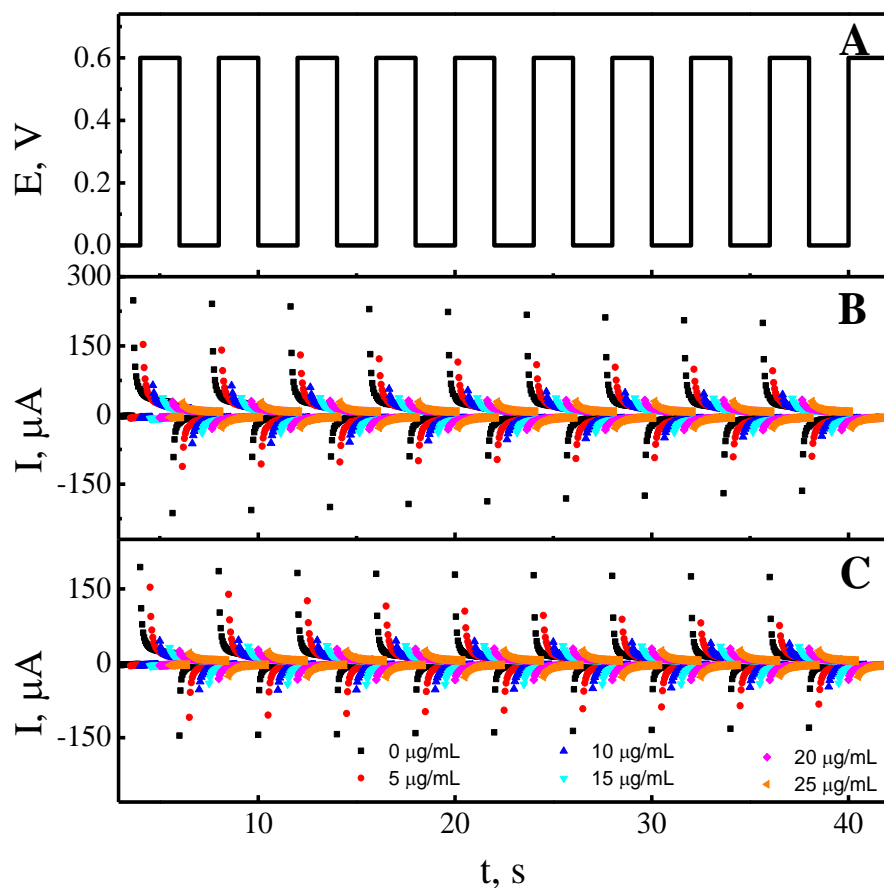
9  
 10 The changes of current at the beginning  $I_1$  and at the end  $I_2$  of pulses of the potential at  
 11 +950 mV are presented in figure 2E. The current changes were not the object of analysis at the  
 12 potential of 0 V, because during this potential step the equilibration of monomer and template  
 13 molecule concentrations in the neighborhood of the working electrode is happening. Previous  
 14 studies demonstrated that the self-assembly of monomers and template molecules due to the  
 15 interactions under thermodynamic control prior to polymerization, is significant for the



1 recognition characteristics of the final polymers [57]. Polymerization of Ppy occurs during the  
2 pulses at a potential value of +950 mV. Therefore, only an insignificant Faradaic process was  
3 observed on the electrode at the 0 V potential step. Thus, the current changes during the  
4 potential step when the potential was elevated up to +950 mV were analyzed more in detail.  
5 For the visualization of the current changes during the electrochemical deposition of Ppy layer  
6 from polymerization solution containing SARS-CoV-2-S glycoprotein and Ppy layer from  
7 polymerization solution non-containing SARS-CoV-2-S glycoprotein two current points at the  
8 beginning  $I_1$  and end  $I_2$  of each potential step were taken into account (Fig. 2D). The comparison  
9 of the current changes demonstrated that the current registered during deposition Ppy layer  
10 from polymerization solution non-containing SARS-CoV-2-S glycoprotein is higher than that  
11 registered during deposition of Ppy layer from polymerization solution containing SARS-CoV-  
12 2-S glycoprotein (Fig. 2E). However, the observed difference of current changes is not very  
13 significant in comparison with that registered in our previous researches [27] and in other  
14 researches [27, 58]. The collation of current changes on Pt electrode during the  
15 electrochemical deposition of Ppy/SARS-CoV-2-S and NIP-Ppy layers have illustrated that  
16 current during the deposition of NIP-Ppy increased just by 1.05 times in comparison to that  
17 registered during the deposition of Ppy/SARS-CoV-2-S. From the current changes observed  
18 during the polymerization, it can be presumed that the entrapped protein molecules just  
19 insignificantly affect the conductivity of the formed layers. During the next MIP-Ppy  
20 preparation step, the entrapped SARS-CoV-2-S glycoprotein were removed from the formed  
21 Ppy/SARS-CoV-2-S layer and MIP-Ppy was formed. In the same way as MIP-Ppy, NIP-Ppy was  
22 also exposed to 0.05 M H<sub>2</sub>SO<sub>4</sub> to eliminate any differences caused by the extraction procedure  
23 on the formed MIP-Ppy, NIP-Ppy layer properties.

24 In the following part of the research, the formed MIP-Ppy and NIP-Ppy layers were  
25 evaluated using pulsed amperometric detection by a sequence of 10 potential pulses of +600 mV  
26 and 0 V for 2 s each as it was suggested in our previous research [42]. Various aspects of  
27 charging-discharging of conducting polymer polypyrrole was well discussed by Heinze et al.  
28 [59]. Also there was stated that overoxidation of the un-substituted Ppy already occurs at 0.65  
29 V vs Ag/AgCl<sub>(3M KCl)</sub> [60]. Hence, taking into account these findings a potential pulse values of 0  
30 V and +600 mV were selected for the determination of SARS-CoV-2-S glycoproteins.

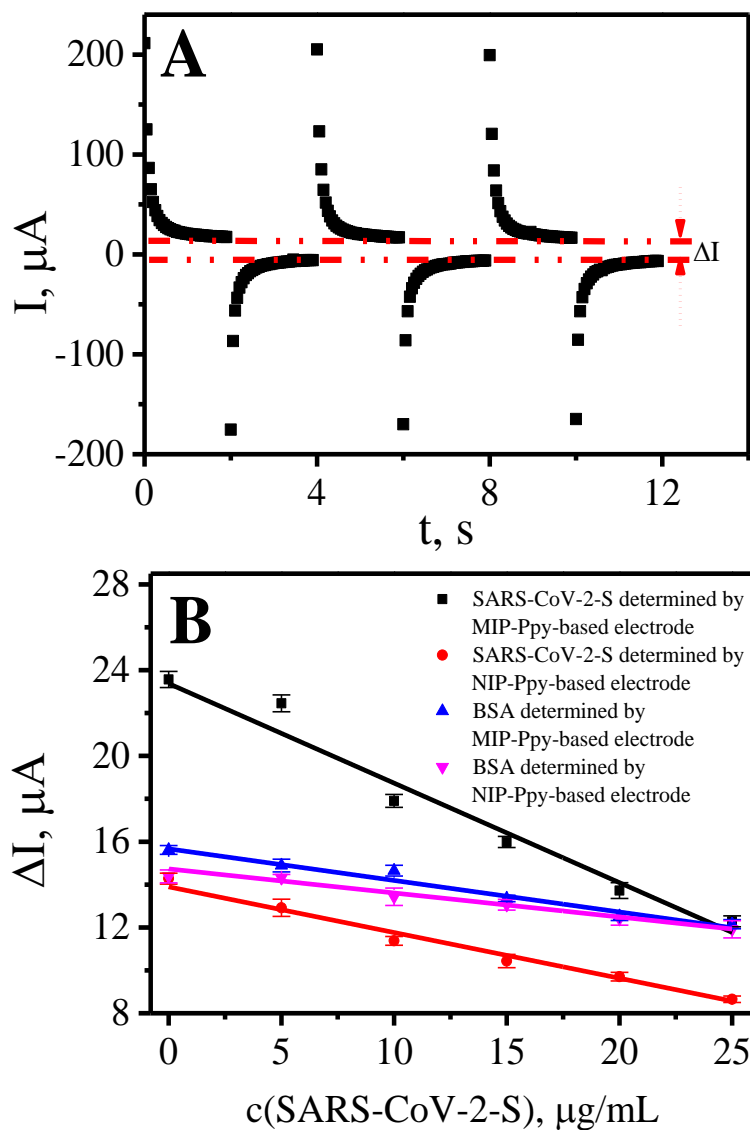
31 The profile of the potential pulse sequence is presented in figure 3A.  
32



1  
 2 **Fig. 3.** Electrochemical evaluation of MIP-Ppy and NIP-Ppy layers was performed by the  
 3 potential pulse sequence. **A** – potential pulse profile. Typical chronoamperograms (during  
 4 pulsed amperometric detection) were obtained at: **B** – MIP-Ppy and **C** – NIP-Ppy modified Pt  
 5 electrode in the absence of SARS-CoV-2-S glycoprotein (▪) and in the presence of SARS-CoV-2-  
 6 S glycoprotein from 5 μg/mL up to 25 μg/mL in PBS solution, pH 7.4 (offset 0.5).

7  
 8 The concentration of SARS-CoV-2-S glycoprotein was varying in the range from 0  
 9 μg/mL to 25 μg/mL. Some other reports described instability of the proteins in presence of  
 10 salts [61, 62], but during the preparation of required concentrations no signs of instability of  
 11 the SARS-CoV-2-S glycoprotein solubilized in PBS were observed. Figures 3B and C  
 12 demonstrate the dependence of the chronoamperometric response (during pulsed  
 13 amperometric detection) of MIP-Ppy and NIP-Ppy Pt electrodes modified with SARS-CoV-2-S  
 14 glycoprotein in the PBS solution. The change in the chronoamperometric response is related  
 15 to the adsorption of less conductive protein molecules on the MIP-Ppy and NIP-Ppy layers.  
 16 When SARS-CoV-2-S glycoprotein concentration in solution was increased, the registered  
 17 chronoamperometric response of both MIP-Ppy and NIP-Ppy-modified Pt electrodes  
 18 decreased. Higher currents were registered before the incubation of electrode in SARS-CoV-2-  
 19 S glycoprotein containing solution. This effect is determined by the presence of water

1 molecules and electrolyte ions in the places where molecular imprints were formed. After the  
 2 incubation in SARS-CoV-2-S glycoprotein containing solution, the ions of solvent and the  
 3 electrolyte were replaced by the molecules of SARS-CoV-2-S glycoprotein and thus the  
 4 registered current at the potential of +600 mV decreased.  
 5  
 6  
 7  
 8  
 9  
 10  
 11



12  
 13 **Fig. 4.** Calibration curves of  $\Delta I$  vs concentration of SARS-CoV-2-S glycoprotein and BSA on MIP-  
 14 Ppy and NIP-Ppy according to the  $\Delta I$  calculated in respect to: **A** – the principal of  $\Delta I$  measuring;

1 **B** –  $\Delta I$ . RSD% was in range from 2 to 4.3% of current values of 5 potential pulses for the listed  
2 data points.

3  
4 **Table 1.** Linear regression characteristics of current ( $\Delta I$ ,  $\mu\text{A}$ ) vs concentration of SARS-CoV-2-  
5 S glycoprotein (c,  $\mu\text{g}/\text{mL}$ ) on the MIP-Ppy and NIP-Ppy modified Pt electrodes.

	$y = ax+b$	a	b	$R^2$
SARS-CoV-2-S determined by MIP-Ppy-based electrode		$-0.46 \pm 0.04$	$23.4 \pm 0.7$	0.96
SARS-CoV-2-S determined by NIP-Ppy-based electrode		$-0.21 \pm 0.01$	$13.9 \pm 0.3$	0.98
BSA determined by MIP-Ppy-based electrode		$-0.15 \pm 0.01$	$15.7 \pm 0.2$	0.97
BSA determined by NIP-Ppy-based electrode		$-0.1 \pm 0.01$	$14.7 \pm 0.1$	0.97

6  
7 The magnitude of current differences, which are registered during potential pulses at  
8 instants when potentials were stepped from 0 mV up to +600 mV and +600 mV down to 0 mV,  
9 has decreased with increasing SARS-CoV-2-S glycoprotein concentration in PBS solution (Fig.  
10 4). Figure 4A represents the current profile, which was registered during potential pulses, and  
11 the way in which the analytical signals ( $\Delta I$ ) for the calibration curve was depicted. According  
12 to this calibration curve, linearity of analytical signal dependence on analyte concentration was  
13 observed at all evaluated SARS-CoV-2-S glycoprotein concentrations in the range from 0  
14  $\mu\text{g}/\text{mL}$  to 25  $\mu\text{g}/\text{mL}$ .

15 The slope derived using the linear regression equation for the changes of current ( $\Delta I$ ,  
16  $\mu\text{A}$ ) vs concentration of SARS-CoV-2-S glycoprotein (c,  $\mu\text{g}/\text{mL}$ ) registered by NIP-Ppy-modified  
17 Pt electrode was of  $-0.22 \mu\text{A}/(\mu\text{g}/\text{mL})$  with  $R^2 = 0.98$  (Table 1). While the slope of linear  
18 regression for the Pt electrode modified with SARS-CoV-2-S glycoprotein imprinted MIP-Ppy  
19 was  $-0.47 \mu\text{A}/(\mu\text{g}/\text{mL})$  with  $R^2 = 0.96$  (Table 1). The sensitivity calculated from the calibration  
20 curves of the MIP-Ppy modified Pt electrode towards SARS-CoV-2-S glycoprotein in the linear  
21 dependence interval according to the  $\Delta I$  measurements was approximately 2.1 times higher  
22 than that of NIP-Ppy modified Pt electrode. This difference is significant and therefore can be  
23 applied in the design of sensors based on MIP-Ppy modified Pt electrodes.

24 The same MIP-Ppy and NIP-Ppy modified Pt electrodes were evaluated for the  
25 interaction with BSA (Fig. 4B) to evaluate the selectivity of MIP-Ppy layer towards different  
26 proteins. The slope values for these measurements were derived using linear regression and  
27 they are represented in Table 1. The slope value ( $-0.15 \mu\text{A}/(\mu\text{g}/\text{mL})$ ) registered by the MIP-  
28 Ppy modified Pt electrodes incubated in BSA containing solution was significantly lower.

1 The comparison of the sensitivity/selectivity results among studies, which are  
2 reporting MIPs sensors based on the different polymers is rather complicated, because several  
3 factors are playing an important role on the final result: (i) the design of the electrochemical  
4 cell, (ii) the electrochemical method used for evaluation of the sensor, (iii) nature of the  
5 polymer, etc.

6 There are published only very few studies concerning the application of molecular  
7 imprinting technology for the analysis of SARS-CoV-2 proteins. There was described the  
8 application study of o-phenylenediamine deposited on the macroporous gold screen-printed  
9 electrode with the receptor-binding domain of SARS-CoV-2-RBD for impedimetric  
10 measurements [55]. The described sensor was sensitive to the concentrations of SARS-CoV-2-  
11 RBD molecules in the range of pg/mL. In another study m-phenylenediamine (mPD) was  
12 imprinted with SARS-CoV-2 nucleoprotein (ncovNP). The sensitivity of the sensor according to  
13 the DPV signal was in the range of fM [54]. In purpose to demonstrate the selectivity of the  
14 sensor BSA and some more proteins were used in the study. The Ppy was imprinted with *gp51*  
15 and was applied in the design of electrochemical sensor [42]. The sensitivity of the sensor  
16 according to the results of simplified pulsed amperometric detection was in the range of  
17  $\mu\text{g/mL}$ . The electrochemical sensors based on Ppy with imprints of prostate-specific antigen  
18 (PSA) was reported in 2020 [15]. The square wave voltammetry technique was used to  
19 determinate PSA concentration. The described sensor was sensitive to the concentrations of  
20 PSA molecules in the range of pg/mL. The electrochemical MIP sensor based on Ppy and  
21 aminophenylboronic acid (p-APBA) bilayer was imprinted with lysozyme [46]. The sensitivity  
22 of the sensor according to the CV signal was in the range of ppm. Hence, several factors govern  
23 the sensitivity of the MIP sensors. The electrochemical method of chronoamperometry (pulsed  
24 amperometric detection) by the sequence of potential pulses was only occasionally used in  
25 previous studies. In present our study, it was demonstrated that the obtained MIP-Ppy  
26 modified Pt electrodes can be applied for the determination of imprinted SARS-CoV-2-S  
27 glycoproteins.

## 28 29 **Conclusions**

30 Pt electrode was modified by two types of Ppy layers: (i) MIP-Ppy layer, which was modified  
31 by imprints of SARS-CoV-2-S glycoprotein and (ii) NIP-Ppy, which was formed without the  
32 imprint of any proteins. The comparison of the current changes on Pt electrode during the  
33 electrochemical deposition of MIP-Ppy and NIP-Ppy has demonstrated that the current for NIP-  
34 Ppy increased approximately by only 1.05 times more than that registered during the

1 deposition of MIP-Ppy layer. This means that the SARS-CoV-2-S glycoprotein, which serves as  
2 the template molecule for MIP-Ppy layer, does not have a crucial effect on the thickness of the  
3 deposited polymer layer and the initial characteristics of the formed MIP-Ppy and NIP-Ppy  
4 layers are comparable.

5 The comparison of calibration curves registered after the incubation of MIP-Ppy and  
6 NIP-Ppy modified Pt electrodes revealed that the interaction of SARS-CoV-2-S glycoprotein  
7 with MIP-Ppy generates 2.1 times higher change of current for MIP-Ppy modified electrode, in  
8 comparison with that registered for NIP-Ppy modified Pt electrode. The selectivity of SARS-  
9 CoV-2-S imprinted MIP-Ppy modified Pt electrode was tested in comparison to BSA solution.  
10 The obtained slope values during the evaluation of MIP-Ppy modified Pt electrode sensitivity  
11 towards BSA were significantly lower when compared with that towards SARS-CoV-2-S  
12 glycoprotein. The results of application of MIP-Ppy modified Pt electrodes demonstrated  
13 higher current changes in respect can be applied for selective determination of the imprinted  
14 SARS-CoV-2-S glycoprotein. Therefore, it can be concluded that the molecular imprinting of the  
15 conducting polymer might be applied for the development of the electrochemical sensor for  
16 the detection of SARS-CoV-2-S glycoprotein.

17

#### 18 **Declaration of interest**

19 The authors declare that they have no known competing financial interests or personal  
20 relationships that could have appeared to influence the work reported in this paper.

21

#### 22 **CRedit authorship contribution statement:**

23

24 **Vilma Ratautaite** – Methodology, Investigation, Data analysis, Writing - original draft,  
25 Interpretation of data, Data analysis;

26 **Raimonda Boguzaitė** – Methodology, Investigation, Data analysis, Writing - original draft,  
27 Interpretation of data, Data analysis;

28 **Ernestas Brazys** – Methodology, Investigation, Data analysis, Writing - original draft,  
29 Interpretation of data, Data analysis;

30 **Almira Ramanaviciene** – Writing - review & editing, Data analysis, Interpretation of data;

31 **Evaldas Ciplys** – Production of protein;

32 **Mindaugas Juozapaitis** – Production of protein;

33 **Rimantas Slibinskas** – Production of protein;

34 **Mikhael Bechelany** – Writing - review & editing;

- 1 **Arunas Ramanavicius** – Interpretation of data, Data analysis, Supervision, Conceptualization,
- 2 Writing - review & editing, Funding acquisition.
- 3
- 4
- 5
- 6
- 7
- 8
- 9
- 10

1  
2  
3  
4  
5  
6  
7  
8  
9  
10  
11  
12  
13  
14  
15  
16  
17  
18  
19  
20  
21  
22  
23  
24  
25  
26  
27  
28  
29  
30  
31  
32  
33  
34  
35  
36  
37  
38  
39  
40  
41  
42  
43  
44  
45  
46

## Acknowledgement

This project has received funding from the Research Council of Lithuania (LMTLT), agreement No S-LZ-21-4 and has been performed in a cooperation with Institut Européen des Membrane, Montpellier University 2, France. Dear Mikhael please check this position how we need to provide correct acknowledgement?

## References

[1] B. Shan, Y.Y. Broza, W. Li, Y. Wang, S. Wu, Z. Liu, J. Wang, S. Gui, L. Wang, Z. Zhang, W. Liu, S. Zhou, W. Jin, Q. Zhang, D. Hu, L. Lin, Q. Zhang, W. Li, J. Wang, H. Liu, Y. Pan, H. Haick, Multiplexed Nanomaterial-Based Sensor Array for Detection of COVID-19 in Exhaled Breath, *ACS Nano*, 14 (2020) 12125-12132.

[2] R.D. Lamboll, C.D. Jones, R.B. Skeie, S. Fiedler, B.H. Samset, N.P. Gillett, J. Rogelj, P.M. Forster, Modifying emission scenario projections to account for the effects of COVID-19: protocol for Covid-MIP, *Geoscientific model development discussions*, 2020 (2020) 1-20.

[3] D. Wu, T. Wu, Q. Liu, Z. Yang, The SARS-CoV-2 outbreak: What we know, *International Journal of Infectious Diseases*, 94 (2020) 44-48.

[4] T. Koyama, D. Platt, L. Parida, Variant analysis of SARS-CoV-2 genomes, *Bull World Health Organ*, 98 (2020) 495-504.

[5] Y.-Z. Zhang, E.C. Holmes, A Genomic Perspective on the Origin and Emergence of SARS-CoV-2, *Cell*, 181 (2020) 223-227.

[6] R.L. Tillett, J.R. Sevinsky, P.D. Hartley, H. Kerwin, N. Crawford, A. Gorzalski, C. Laverdure, S.C. Verma, C.C. Rossetto, D. Jackson, M.J. Farrell, S. Van Hooser, M. Pandori, Genomic evidence for reinfection with SARS-CoV-2: a case study, *The Lancet Infectious Diseases*, 21 (2021) 52-58.

[7] R.J. Rockett, A. Arnott, C. Lam, R. Sadsad, V. Timms, K.-A. Gray, J.-S. Eden, S. Chang, M. Gall, J. Draper, E.M. Sim, N.L. Bachmann, I. Carter, K. Basile, R. Byun, M.V. O'Sullivan, S.C.A. Chen, S. Maddocks, T.C. Sorrell, D.E. Dwyer, E.C. Holmes, J. Kok, M. Prokopenko, V. Sintchenko, Revealing COVID-19 transmission in Australia by SARS-CoV-2 genome sequencing and agent-based modeling, *Nature Medicine*, 26 (2020) 1398-1404.

[8] L. Yurkovetskiy, X. Wang, K.E. Pascal, C. Tomkins-Tinch, T.P. Nyalile, Y. Wang, A. Baum, W.E. Diehl, A. Dauphin, C. Carbone, K. Veinotte, S.B. Egri, S.F. Schaffner, J.E. Lemieux, J.B. Munro, A. Rafique, A. Barve, P.C. Sabeti, C.A. Kyratsous, N.V. Dudkina, K. Shen, J. Luban, Structural and Functional Analysis of the D614G SARS-CoV-2 Spike Protein Variant, *Cell*, 183 (2020) 739-751.e738.

[9] A.C. Walls, Y.-J. Park, M.A. Tortorici, A. Wall, A.T. McGuire, D. Veesler, Structure, Function, and Antigenicity of the SARS-CoV-2 Spike Glycoprotein, *Cell*, 181 (2020) 281-292.e286.

[10] P. Calligari, S. Bobone, G. Ricci, A. Bocedi, Molecular Investigation of SARS-CoV-2 Proteins and Their Interactions with Antiviral Drugs, *Viruses*, 12 (2020) 445.

[11] Y. Huang, C. Yang, X.-f. Xu, W. Xu, S.-w. Liu, Structural and functional properties of SARS-CoV-2 spike protein: potential antiviral drug development for COVID-19, *Acta Pharmacologica Sinica*, 41 (2020) 1141-1149.

[12] F. Amanat, F. Krammer, SARS-CoV-2 Vaccines: Status Report, *Immunity*, 52 (2020) 583-589.

[13] B. Hu, H. Guo, P. Zhou, Z.-L. Shi, Characteristics of SARS-CoV-2 and COVID-19, *Nature Reviews Microbiology*, (2020).



- 1 [14] A. Tretjakov, V. Syritski, J. Reut, R. Boroznjak, A. Öpik, Molecularly imprinted polymer film  
2 interfaced with Surface Acoustic Wave technology as a sensing platform for label-free protein  
3 detection, *Analytica Chimica Acta*, 902 (2016) 182-188.
- 4 [15] Z. Mazouz, M. Mokni, N. Fourati, C. Zerrouki, F. Barbault, M. Seydou, R. Kalfat, N. Yaakoubi,  
5 A. Omezzine, A. Bouslema, A. Othmane, Computational approach and electrochemical  
6 measurements for protein detection with MIP-based sensor, *Biosensors and Bioelectronics*,  
7 151 (2020) 111978.
- 8 [16] A. Kidakova, R. Boroznjak, J. Reut, A. Öpik, M. Saarma, V. Syritski, Molecularly imprinted  
9 polymer-based SAW sensor for label-free detection of cerebral dopamine neurotrophic factor  
10 protein, *Sensors and Actuators B: Chemical*, 308 (2020) 127708.
- 11 [17] R. Thoelen, R. Vansweevelt, J. Duchateau, F. Horemans, J. D'Haen, L. Lutsen, D.  
12 Vanderzande, M. Ameloot, M. VandeVen, T.J. Cleij, P. Wagner, A MIP-based impedimetric sensor  
13 for the detection of low-MW molecules, *Biosensors and Bioelectronics*, 23 (2008) 913-918.
- 14 [18] C. Malitesta, E. Mazzotta, R.A. Picca, A. Poma, I. Chianella, S.A. Piletsky, MIP sensors - the  
15 electrochemical approach, *Analytical and Bioanalytical Chemistry*, 402 (2012) 1827-1846.
- 16 [19] A.G. Ayankojo, J. Reut, V. Ciocan, A. Öpik, V. Syritski, Molecularly imprinted polymer-based  
17 sensor for electrochemical detection of erythromycin, *Talanta*, 209 (2020) 120502.
- 18 [20] S. Ansari, S. Masoum, Molecularly imprinted polymers for capturing and sensing proteins:  
19 Current progress and future implications, *TrAC Trends in Analytical Chemistry*, 114 (2019) 29-  
20 47.
- 21 [21] H.F. El-Sharif, D. Stevenson, S.M. Reddy, MIP-based protein profiling: A method for  
22 interspecies discrimination, *Sensors and Actuators B: Chemical*, 241 (2017) 33-39.
- 23 [22] V. Ratautaite, S.D. Janssens, K. Haenen, M. Nešládek, A. Ramanaviciene, I. Baleviciute, A.  
24 Ramanavicius, Molecularly Imprinted Polypyrrole Based Impedimetric Sensor for  
25 Theophylline Determination, *Electrochimica Acta*, 130 (2014) 361-367.
- 26 [23] E.N. Ndunda, Molecularly imprinted polymers—A closer look at the control polymer used  
27 in determining the imprinting effect: A mini review, *Journal of Molecular Recognition*, 33  
28 (2020) e2855.
- 29 [24] O.S. Ahmad, T.S. Bedwell, C. Esen, A. Garcia-Cruz, S.A. Piletsky, Molecularly Imprinted  
30 Polymers in Electrochemical and Optical Sensors, *Trends in Biotechnology*, 37 (2019) 294-309.
- 31 [25] B. Yang, C. Fu, J. Li, G. Xu, *Frontiers in highly sensitive molecularly imprinted*  
32 *electrochemical sensors: Challenges and strategies*, *TrAC Trends in Analytical Chemistry*, 105  
33 (2018) 52-67.
- 34 [26] T. Alizadeh, M.R. Ganjali, M. Zare, P. Norouzi, Development of a voltammetric sensor based  
35 on a molecularly imprinted polymer (MIP) for caffeine measurement, *Electrochimica Acta*, 55  
36 (2010) 1568-1574.
- 37 [27] D. Plausinaitis, L. Sinkevicius, U. Samukaite-Bubniene, V. Ratautaite, A. Ramanavicius,  
38 Evaluation of Electrochemical Quartz Crystal Microbalance Based Sensor Modified by Uric  
39 Acid-imprinted Polypyrrole, *Talanta*, 220 (2020) 121414.
- 40 [28] J.W. Lowdon, H. Diliën, P. Singla, M. Peeters, T.J. Cleij, B. van Grinsven, K. Eersels, MIPs for  
41 commercial application in low-cost sensors and assays – An overview of the current status quo,  
42 *Sensors and Actuators B: Chemical*, 325 (2020) 128973.
- 43 [29] G. Selvolini, G. Marrazza, MIP-Based Sensors: Promising New Tools for Cancer Biomarker  
44 Determination, *Sensors*, 17 (2017) 718.
- 45 [30] V. Ratautaite, D. Plausinaitis, I. Baleviciute, L. Mikoliunaite, A. Ramanaviciene, A.  
46 Ramanavicius, Characterization of Caffeine-Imprinted Polypyrrole by a Quartz Crystal  
47 Microbalance and Electrochemical Impedance Spectroscopy, *Sensors and Actuators B:*  
48 *Chemical*, 212 (2015) 63-71.
- 49 [31] V. Ratautaite, M. Nešládek, A. Ramanaviciene, I. Baleviciute, A. Ramanavicius, Evaluation  
50 of Histamine Imprinted Polypyrrole Deposited on Boron Doped Nanocrystalline Diamond,  
51 *Electroanalysis*, 26 (2014) 2458–2464.

1 [32] M. Dabrowski, P. Lach, M. Cieplak, W. Kutner, Nanostructured molecularly imprinted  
2 polymers for protein chemosensing, *Biosensors and Bioelectronics*, 102 (2018) 17-26.

3 [33] V.K. Tamboli, N. Bhalla, P. Jolly, C.R. Bowen, J.T. Taylor, J.L. Bowen, C.J. Allender, P. Estrela,  
4 Hybrid Synthetic Receptors on MOSFET Devices for Detection of Prostate Specific Antigen in  
5 Human Plasma, *Anal. Chem.*, 88 (2016) 11486-11490.

6 [34] Q. Zeng, X. Huang, M. Ma, A molecularly imprinted electrochemical sensor based on  
7 polypyrrole/carbon nanotubes composite for the detection of S-ovalbumin in egg white,  
8 *International Journal of Electrochemical Science*, 12 (2017) 3965-3981.

9 [35] V.V. Shumyantseva, T.V. Bulko, L.V. Sigolaeva, A.V. Kuzikov, A.I. Archakov, Electrosynthesis  
10 and binding properties of molecularly imprinted poly-o-phenylenediamine for selective  
11 recognition and direct electrochemical detection of myoglobin, *Biosensors and Bioelectronics*,  
12 86 (2016) 330-336.

13 [36] Z. Stojanovic, J. Erdőssy, K. Keltai, F.W. Scheller, R.E. Gyurcsányi, Electrosynthesized  
14 molecularly imprinted polyscopoletin nanofilms for human serum albumin detection,  
15 *Analytica Chimica Acta*, 977 (2017) 1-9.

16 [37] J. Erdőssy, V. Horváth, A. Yarman, F.W. Scheller, R.E. Gyurcsányi, Electrosynthesized  
17 molecularly imprinted polymers for protein recognition, *TrAC Trends in Analytical Chemistry*,  
18 79 (2016) 179-190.

19 [38] A. Yarman, D. Dechtrirat, M. Bossertdt, K.J. Jetzschmann, N. Gajovic-Eichelmann, F.W.  
20 Scheller, Cytochrome c-Derived Hybrid Systems Based on Molecularly Imprinted Polymers,  
21 *Electroanalysis*, 27 (2015) 573-586.

22 [39] L.-W. Qian, X.-L. Hu, P. Guan, B. Gao, D. Wang, C.-L. Wang, J. Li, C.-B. Du, W.-Q. Song, Thermal  
23 preparation of lysozyme-imprinted microspheres by using ionic liquid as a stabilizer,  
24 *Analytical and Bioanalytical Chemistry*, 406 (2014) 7221-7231.

25 [40] S. Wu, W. Tan, H. Xu, Protein molecularly imprinted polyacrylamide membrane: for  
26 hemoglobin sensing, *Analyst*, 135 (2010) 2523-2527.

27 [41] A. Tlili, G. Attia, S. Khaoulani, Z. Mazouz, C. Zerrouki, N. Yaakoubi, A. Othmane, N. Fourati,  
28 Contribution to the Understanding of the Interaction between a Polydopamine Molecular  
29 Imprint and a Protein Model: Ionic Strength and pH Effect Investigation, *Sensors*, 21 (2021)  
30 619.

31 [42] A. Ramanaviciene, A. Ramanavicius, Molecularly imprinted polypyrrole-based synthetic  
32 receptor for direct detection of bovine leukemia virus glycoproteins, *Biosensors and*  
33 *Bioelectronics*, 20 (2004) 1076-1082.

34 [43] I. Baleviciute, V. Ratautaite, A. Ramanaviciene, Z. Balevicius, J. Broeders, D. Croux, M.  
35 McDonald, F. Vahidpour, R. Thoelen, W.D. Ceuninck, K. Haenen, M. Nesladek, A. Reza, A.  
36 Ramanavicius, Evaluation of theophylline imprinted polypyrrole film, *Synth. Met.*, 209 (2015)  
37 206-211.

38 [44] V. Ratautaite, S.N. Topkaya, L. Mikoliunaite, M. Ozsoz, Y. Oztekin, A. Ramanaviciene, A.  
39 Ramanavicius, Molecularly Imprinted Polypyrrole for DNA Determination *Electroanalysis* 25  
40 (2013) 1169-1177.

41 [45] R. Viter, K. Kunene, P. Genys, D. Jevdokimovs, D. Erts, A. Sutka, K. Bisetty, A. Viksna, A.  
42 Ramanaviciene, A. Ramanavicius, Photoelectrochemical Bisphenol S Sensor Based on ZnO-  
43 Nanoroads Modified by Molecularly Imprinted Polypyrrole, *Macromolecular Chemistry and*  
44 *Physics*, 221 (2020) 1900232.

45 [46] J. Rick, T.-C. Chou, Amperometric protein sensor – fabricated as a polypyrrole, poly-  
46 aminophenylboronic acid bilayer, *Biosensors and Bioelectronics*, 22 (2006) 329-335.

47 [47] X. Kan, Z. Xing, A. Zhu, Z. Zhao, G. Xu, C. Li, H. Zhou, Molecularly imprinted polymers based  
48 electrochemical sensor for bovine hemoglobin recognition, *Sensors and Actuators B: Chemical*,  
49 168 (2012) 395-401.

- 1 [48] H.-J. Chen, Z.-H. Zhang, L.-J. Luo, S.-Z. Yao, Surface-imprinted chitosan-coated magnetic  
2 nanoparticles modified multi-walled carbon nanotubes biosensor for detection of bovine  
3 serum albumin, *Sensors and Actuators B: Chemical*, 163 (2012) 76-83.
- 4 [49] M.L. Yola, N. Atar, Development of cardiac troponin-I biosensor based on boron nitride  
5 quantum dots including molecularly imprinted polymer, *Biosensors and Bioelectronics*, 126  
6 (2019) 418-424.
- 7 [50] B.V.M. Silva, B.A.G. Rodríguez, G.F. Sales, M.D.P.T. Sotomayor, R.F. Dutra, An ultrasensitive  
8 human cardiac troponin T graphene screen-printed electrode based on electropolymerized-  
9 molecularly imprinted conducting polymer, *Biosensors and Bioelectronics*, 77 (2016) 978-  
10 985.
- 11 [51] Z. Wang, F. Li, J. Xia, L. Xia, F. Zhang, S. Bi, G. Shi, Y. Xia, J. Liu, Y. Li, L. Xia, An ionic liquid-  
12 modified graphene based molecular imprinting electrochemical sensor for sensitive detection  
13 of bovine hemoglobin, *Biosensors and Bioelectronics*, 61 (2014) 391-396.
- 14 [52] L. Li, L. Yang, Z. Xing, X. Lu, X. Kan, Surface molecularly imprinted polymers-based  
15 electrochemical sensor for bovine hemoglobin recognition, *Analyst*, 138 (2013) 6962-6968.
- 16 [53] O.I. Parisi, M. Dattilo, F. Patitucci, R. Malivindi, V. Pezzi, I. Perrotta, M. Ruffo, F. Amone, F.  
17 Puoci, "Monoclonal-type" plastic antibodies for SARS-CoV-2 based on Molecularly Imprinted  
18 Polymers, *bioRxiv*, (2020) 2020.2005.2028.120709.
- 19 [54] A. Raziq, A. Kidakova, R. Boroznjak, J. Reut, A. Öpik, V. Syritski, Development of a portable  
20 MIP-based electrochemical sensor for detection of SARS-CoV-2 antigen, *Biosensors and*  
21 *Bioelectronics*, 178 (2021) 113029.
- 22 [55] M.A. Tabrizi, J.P. Fernández-Blázquez, D.M. Medina, P. Acedo, An ultrasensitive  
23 molecularly imprinted polymer-based electrochemical sensor for the determination of SARS-  
24 CoV-2-RBD by using macroporous gold screen-printed electrode, *Biosensors and*  
25 *Bioelectronics*, (2021) 113729.
- 26 [56] A. Ramanavicius, Y. Oztekin, A. Ramanaviciene, Electrochemical formation of polypyrrole-  
27 based layer for immunosensor design, *Sensors and Actuators B: Chemical*, 197 (2014) 237-  
28 243.
- 29 [57] J. Svenson, H.S. Andersson, S.A. Piletsky, I.A. Nicholls, Spectroscopic studies of the  
30 molecular imprinting self-assembly process, *Journal of Molecular Recognition*, 11 (1998) 83-  
31 86.
- 32 [58] N. Ermis, N. Tinkilic, Preparation of Molecularly Imprinted Polypyrrole Modified Gold  
33 Electrode for Determination of Tyrosine in Biological Samples, *International Journal of*  
34 *Electrochemical Science*, 13 (2018) 2286-2298.
- 35 [59] J. Heinze, B.A. Frontana-Uribe, S. Ludwigs, Electrochemistry of Conducting Polymers—  
36 Persistent Models and New Concepts, *Chemical Reviews*, 110 (2010) 4724-4771.
- 37 [60] T.W. Lewis, G.G. Wallace, C.Y. Kim, D.Y. Kim, Studies of the overoxidation of polypyrrole,  
38 *Synth. Met.*, 84 (1997) 403-404.
- 39 [61] J.N. de Wit, T.v. Kessel, Effects of ionic strength on the solubility of whey protein products.  
40 A colloid chemical approach, *Food Hydrocolloids*, 10 (1996) 143-149.
- 41 [62] D.L. Beauchamp, M. Khajepour, Studying salt effects on protein stability using  
42 ribonuclease t1 as a model system, *Biophysical Chemistry*, 161 (2012) 29-38.
- 43